ELSEVIER

Dyes and Pigments 41 (1999) 211–220

DYES and PIGMENTS

Oxidative degradation of dyes by ultraviolet radiation in the presence of hydrogen peroxide

Gian Maria Colonna [a], Tullio Caronna [b], Bruno Marcandalli [a,*]

[a] *Stazione sperimentale per la Seta,Via G.Colombo 81, I-20133 Milano, Italy*
[b] *Dipartimento di Chimica, Politecnico di Milano, Milano, Italy*

Received 5 October 1998; accepted 4 November 1998

Abstract

The decolorization and mineralization of some azo and anthraquinone dyes by photoactivated hydrogen peroxide has been studied. The degradation process seems to occur according to a similar mechanism for all the selected dyes. Decolorization is complete in a relatively short time and follows apparent first order kinetics, whereas mineralization requires longer irradiation times. Initially fluorescent intermediates are generated in all cases by hydroxylation of the studied compounds. A simple kinetic model, describing adequately the process, has been proposed; pH does not influence significantly the process in the range going from 3 to 9. © 1999 Elsevier Science Ltd. All rights reserved.

Keywords: Azo dyes; Anthraquinone dyes; Advanced oxidation processes; Decolorization

1. Introduction

Textile finishing mills discharge wastewater containing a great variety of organic contaminants in a wide range of concentrations. Many of these compounds are hard to treat by conventional activated sludge systems and may be finally released to the environment.

Coagulation/flocculation, activated carbon adsorption or membrane techniques can only transfer, more or less effectively, the contaminants from one phase to another, leaving the final environmental problem unsolved. Therefore, it is more and more necessary to develop destructive systems leading to complete mineralization or, at least, to less harmful or easy-to-treat compounds. From this point of view, oxidation of organic pollutants is an attractive method. However, the direct reaction of organic compounds with oxygen requires very high temperatures and involves high costs.

During the last decade a series of new methods for water and wastewater purification, the so-called Advanced Oxidation Processes (AOPs), have received considerable attention [1–4]. They have been defined as near ambient temperature processes involving the generation of short-lived, highly oxidative species, especially the hydroxyl radical (redox potential = 2.8 V) [2]. In principle, AOPs are characterized by high oxidation rates, flexibility, small dimension of the equipment and easy adaptability to water recycling processes. The main drawbacks are high operating costs, the need of specialized operators and more stringent safety

* Corresponding author. Tel.: +39-02-7063-5047; fax: +39-2362-788.

0143-7208/99/$ - see front matter
PII: S0143-7208(98)00085-0

requirements because of the use of very reactive chemicals or high-energy sources. The possibility of formation of toxic intermediates, should also be considered if the process is not completed. Currently, due to the high costs and the experimental difficulties in attaining complete mineralization of systems such as industrial wastewater, these methods seem better suited as a preliminary step, carried out directly in the mill, of a subsequent biological treatment or as a part of a process that involves complete or partial water re-use.

In comparison with other AOPs, such as Fenton, ozone, UV/O_3, UV/TiO_2, etc. , the photolysis of hydrogen peroxide shows some advantages such as the complete miscibility of H_2O_2 with water, the stability and commercial availability of hydrogen peroxide, no phase transfer problems, no sludge formation, simplicity of operation and lower investment costs.

Photolysis of hydrogen peroxide is a very simple reaction running with high efficiency:

$$H_2O_2 \xrightarrow{h\nu} 2\,^{\bullet}OH$$

Unfortunately, the molar absorptivity of hydrogen peroxide is rather low in the readily accessible UV-region. The absorption spectrum exhibits a slow and steady rise from 400 nm to 185 nm and, at 254 nm the molar absorptivity is about 19 l mol^{-1} cm^{-1} [5].

The hydroxyl radicals generated by H_2O_2 photolysis in the presence of organic compounds may give rise to different reactions, such as:

1. hydrogen abstraction

$$RH + {}^{\bullet}OH \rightarrow R^{\bullet} + H_2O$$

2. electrophile addition

$$HO^{\bullet} + PhX \rightarrow HOPhX^{\bullet}$$

3. electron transfer

$$HO\bullet + RX \rightarrow RX^{\bullet +} + HO^{-}$$

The radical species formed through the above reactions give rise to further reactions leading finally, under favourable conditions, to complete mineralization.

In the present paper we have selected the UV photolysis of H_2O_2 as a source of hydroxyl radicals and investigated the decolorization and mineralization of some model dyes of different classes as a first step of a research aimed at evaluating the applicability of this technique to the treatment and re-use of dyehouse wastewater.

2. Experimental

2.1. Reagents

Analytical grade 30% H_2O_2 (Carlo Erba, Italy), free from inhibitors, was used without further purification. Water was purified by means of a Millipore (MilliQ®) system.

The dyes used in this study were obtained from Sigma Aldrich. Prior to use, they were Soxhlet extracted with hexane or petroleum ether (e.p. 40–60°C) and subsequently recrystallized from methanol. All dye/water solutions were found to follow Lambert–Beer law in the concentration range from 1×10^{-5} M to 1×10^{-3} M.

All the other reagents were at reagent grade quality (Carlo Erba , Italy) and were used as received.

2.2. Apparatus and methods

The photochemical experiments were carried out at room temperature (20°C ± 2°C), in batch mode, in a 1.5 ℓ immersion photoreactor. The radiation source was a water-jacketed medium pressure mercury UV lamp (500 W according to the manufacturer) (Italquartz, Italy). The radiation flux was measured by hydrogen peroxide actinometry, according to Nicole et al. [5], before each experimental test. The impinging flux, in the UV region where H_2O_2 absorbs, was found to range from 2.1×10^{-6} einstein ℓ^{-1} s^{-1} to 2.9×10^{-6} einstein l^{-1} s^{-1}. Dye concentration for the degradation experiments was 2.5×10^{-4} M for each dye. This value was chosen as a compromise between the necessity to limit internal optical

filter effects and that to adequately follow the kinetic runs.

At desired time intervals, aliquots of the test solution were sampled, and immediately analyzed for dye and TOC concentrations, as well as for fluorometric measurements. Special runs were carried out for the monitoring of other species. The temperature of the irradiated solutions was checked continuously and found to be practically constant, rising only 2°C in 60 min.

The rate of disappearance of a given dye was monitored spectrophotometrically at the visible maximum absorption wavelength. A UV/VIS Perkin Elmer Lambda 15 instrument was used, while fluorescence measurements were effected by means of a Spex Fluorolog apparatus.

Hydrogen peroxide concentration was determined by absorption spectrophotometry at 410 nm of the complex formed with Ti(IV) (Perextest®–Merck) [6]. Total Organic Carbon (TOC) content was measured by means of a Shimadzu TOC 5000 apparatus. Anion analysis was carried out by means of a Waters 600 HPLC instrument equipped with a IC PAK A Waters column and a conductimetric detector (Waters 431®). A borate/gluconate buffer (pH 8.5) was used as eluent.

Solutions to be photolyzed were prepared immediately before irradiation. Control experiments were performed to investigate loss of probe compounds in irradiated systems containing no H_2O_2 and in solutions containing H_2O_2, but kept in the dark.

3. Results and discussion

The dyes chosen for this study are reported in Figs. 1 and 2. AR1, AR40 and MO are azo compounds, while RB19, AB25, AG27 and AB80 are anthraquinone dyes.

The degradation behaviour of AR1, AR40 and MO is shown in Fig. 3 and that of RB19, AB25, AG27 and AB80 in Figs. 4 and 5. Figs. 6 and 7 show the corresponding TOC changes with time. The experiments reported in the above figures were carried out with a $[H_2O_2]/[dye]$ ratio of 40. The disappearance of colour was always accompanied by the formation of fluorescent species, as shown

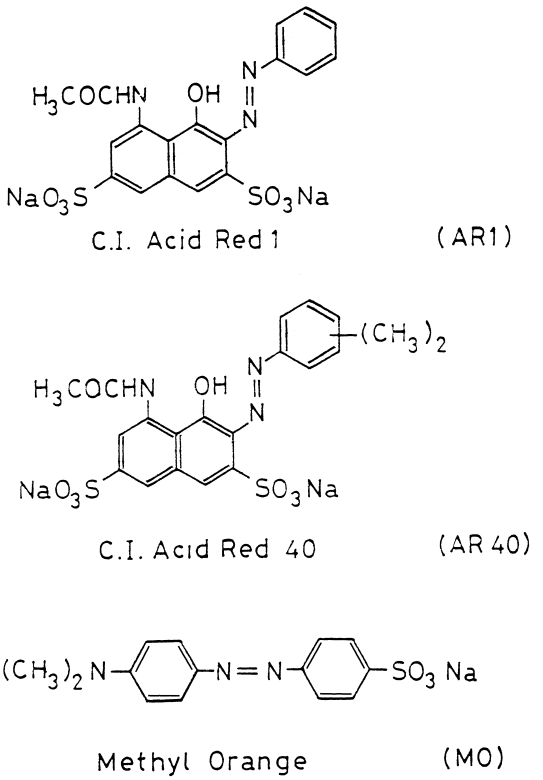

Fig. 1. Structure of dyes AR1, AR40 and MO.

in Figs. 3–5; emission of these species goes through a maximum and, finally, rapidly decays.

TOC vs time plots show that, after an initial period of constant or slowly decreasing values, a relatively rapid decrease occurs. Generally, this final step towards complete mineralization starts only when decolorization is almost complete and fluorescent emission decay is in an initial stage. In all cases at least 90% mineralization was obtained in no more than 3 h. The process leads to TOC disappearance only if it is carried out under irradiation. If irradiation is stopped, at whatever stage, the test solution may be maintained in the dark for some days at room temperature without showing any noticeable change.

Blank tests have shown that no dye photodegradation occurred in the absence of hydrogen peroxide and no oxidation in the absence of irradiation, under the adopted experimental conditions. This qualitative description is common to all the dyes taken into consideration.

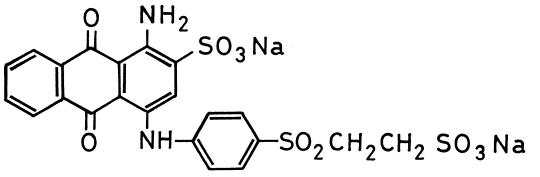

C.I. Reactive Blue 19 (RB 19)

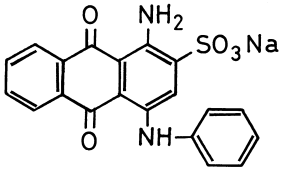

C.I. Acid Blue 25 (AB 25)

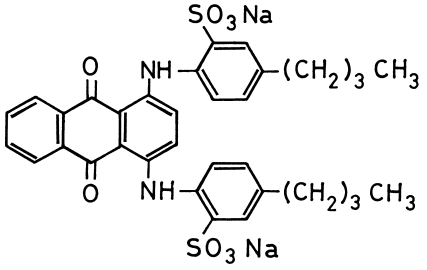

C.I. Acid Green 27 (AG 27)

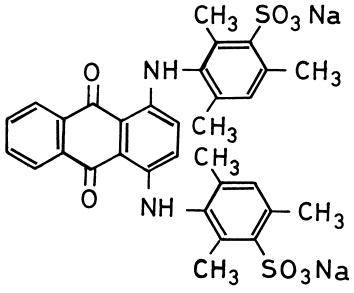

C.I. Acid Blue 80 (AB 80)

Fig. 2. Structure of dyes RB19, AB25, AG27 and AB80.

The observed behaviour can be interpreted by assuming that initial hydroxyl radical attack leads to intermediates which maintain an aromatic structure and may exhibit fluorescence, even if the chromogenic structure is altered or destroyed. Subsequently, further reactions with hydroxyl radicals and/or thermal or photochemical processes lead to smaller organic molecules which are finally completely mineralized.

The behaviour described above may be interpreted quantitatively by the following simplified kinetic model:

$$H_2O_2 \xrightarrow{h\nu} 2\,{}^{\bullet}OH$$

$$\text{Dye} + HO^{\bullet} \xrightarrow{k_1} \text{Int}$$

$$\text{Int} + HO^{\bullet} \xrightarrow{k_2} P_1$$

$$P_1 \underset{k_3}{\overset{h\nu}{\rightarrow}} P_2$$

Due to the fact that hydroxyl radical attack may involve the formation of a complex mixture of different products, and that their individual identification or quantification was not the aim of this work, **Int** and $\mathbf{P_1}$ represent, globally, generic intermediates, some of which exhibit fluorescent emission. This scheme is in agreement with the mechanism of oxidative degradation of other organic compounds brought about by UV/H_2O_2 [7–12].

The corresponding kinetic equations are:

$$-\mathrm{d}[H_2O_2]/\mathrm{d}t = 2\phi I_a \tag{1}$$

$$-\mathrm{d}[\text{dye}]/\mathrm{d}t = k_1[\text{dye}][\text{OH}] \tag{2}$$

$$-\mathrm{d}[\text{OH}]/\mathrm{d}t = k_1[\text{dye}][\text{OH}] + k_2[\text{Int}][\text{OH}] - 2\phi I_a \tag{3}$$

$$-\mathrm{d}[\text{Int}]/\mathrm{d}t = k_2[\text{Int}][\text{OH}] - k_1[\text{dye}][\text{OH}] \tag{4}$$

$$-\mathrm{d}[P_1]/\mathrm{d}t = -k_2[\text{Int}][\text{OH}] + k_3[P_1] \tag{5}$$

$$\mathrm{d}[P_2]/\mathrm{d}t = k_3[P_1] \tag{6}$$

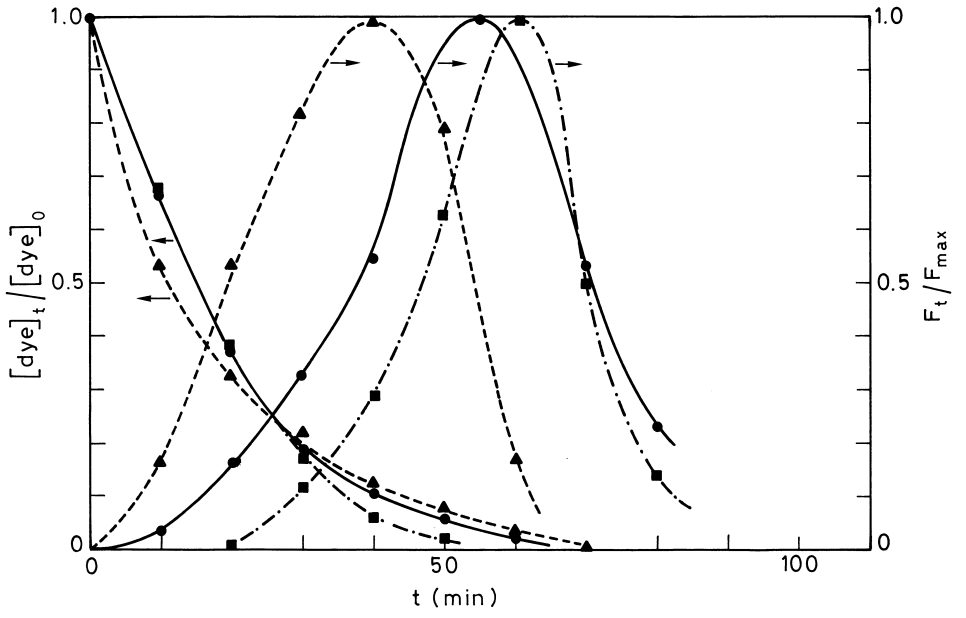

Fig. 3. Comparison of decolorization and fluorescent behaviour of AR1 (—▲—), AR40 (__●__) and MO (---■---) by hydrogen peroxide under UV irradiation as a function of time. F_t: emission intensity at 450 nm (excitation wavelength = 366 nm); F_{max}: maximum emission intensity registered during the kinetic run for each dye. $[H_2O_2]/[dye]_o = 40$. $[dye]_o = 2.5 \times 10^{-4}$ M.

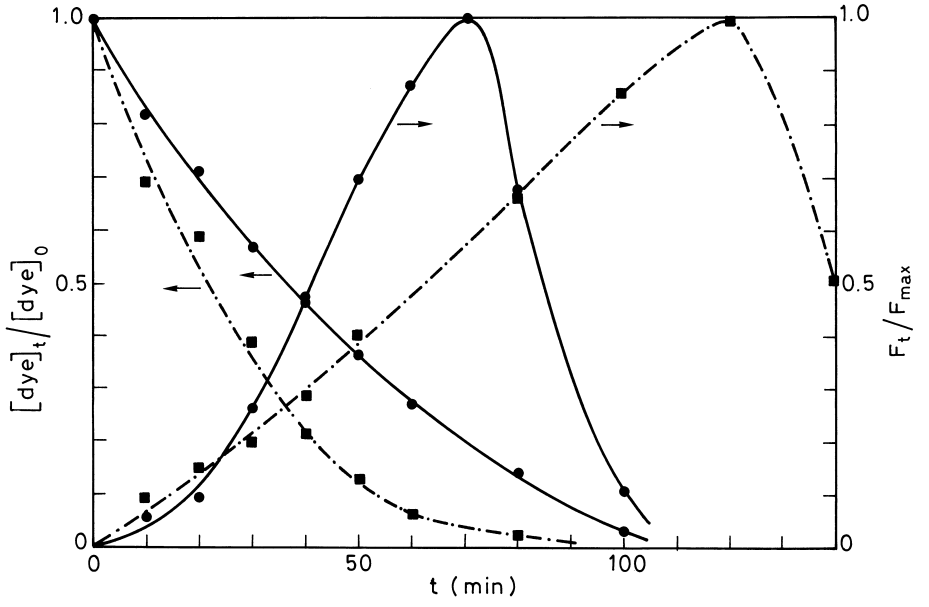

Fig. 4. Comparison of decolorization and fluorescent behaviour of AB25 (-●-) and AB80 (-■-) by hydrogen peroxide under UV irradiation as a function of time. F_t: emission intensity at 460 nm (excitation wavelength = 360 nm); F_{max}: maximum emission intensity registered during the kinetic run for each dye. $[H_2O_2]/[dye]_o = 40$. $[dye]_o = 2.5 \times 10^{-4}$ M.

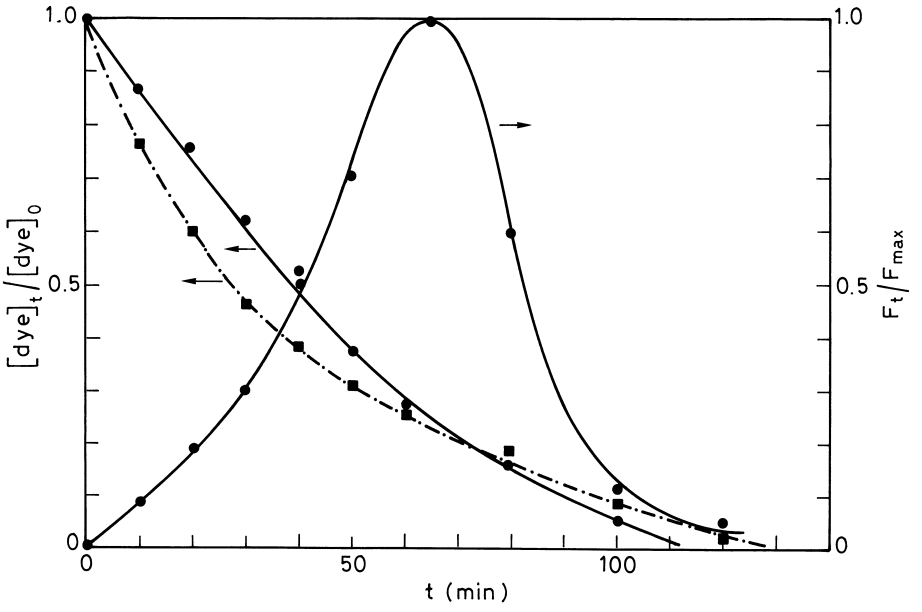

Fig. 5. Comparison of decolorization and fluorescent behaviour of RB19 (-●-) and AG27 (-■-) by hydrogen peroxide under UV irradiation as a function of time. F_t: emission intensity at 460 nm (excitation wavelength = 360 nm); F_{max}: maximum emission intensity registered during the kinetic run for each dye. $[H_2O_2]/[dye]_o = 40$. $[dye]_o = 2.5 \times 10^{-4}$ M.

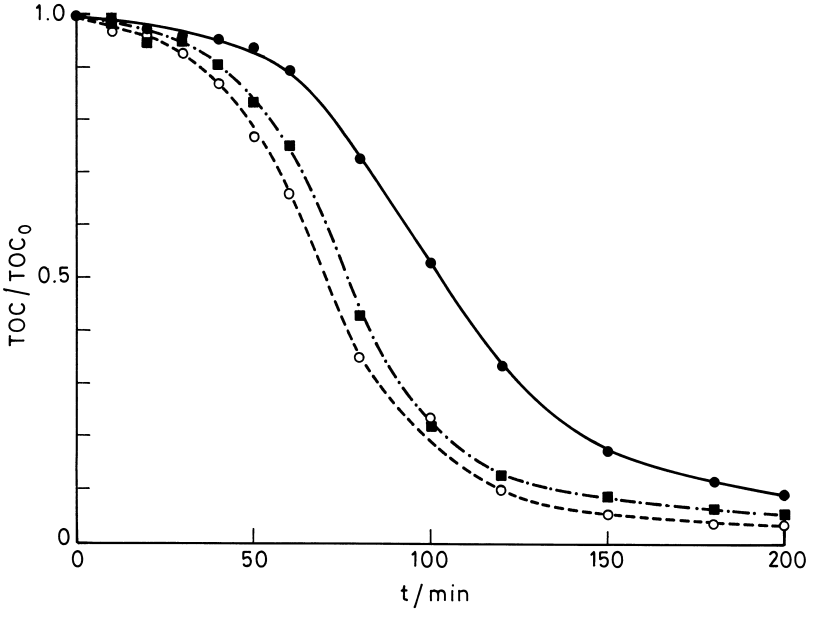

Fig. 6. Relative TOC vs time profile of AR1 (–○—), AR40 (-●-) and MO (---■---) exposed to UV radiation in the presence of hydrogen peroxide. $[H_2O_2]/[dye]_o = 40$. $[dye]_o = 2.5 \times 10^{-4}$ M.

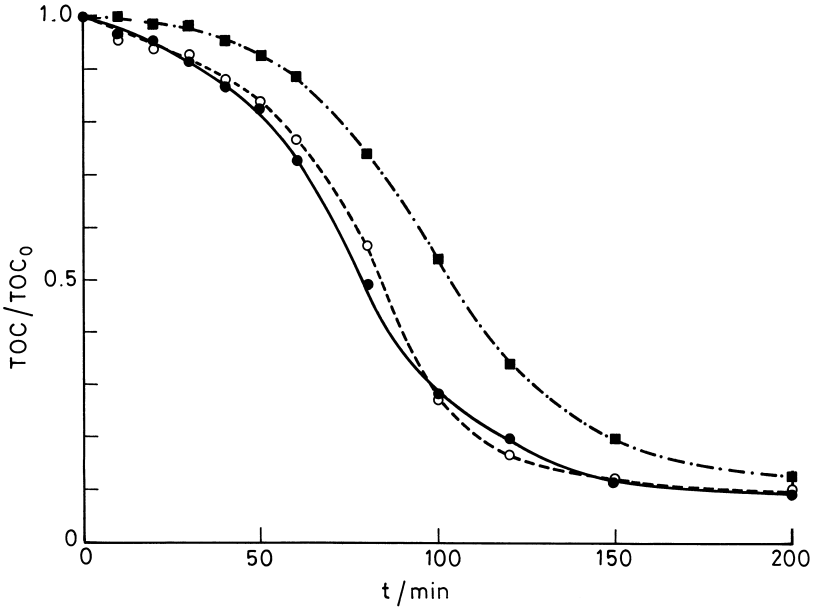

Fig. 7. Relative TOC vs time profile of RB19 (-●-), AB25 (–○—) and AB80 (---■---) exposed to UV radiation in the presence of hydrogen peroxide. $[H_2O_2]/[dye]_o = 40$. $[dye]_o = 2.5\times10^{-4}$ M.

where ϕ is the quantum yield of the photochemical dissociation of hydrogen peroxide, I_a is the radiation intensity absorbed by H_2O_2 and, for simplicity, OH is used to indicate the hydroxyl radical.

If only the early stages of the process are considered, when only **Int** and **dye** may be assumed to be present in the test solution, the following relationship is obtained by applying steady state approximation to [OH]:

$$-\mathrm{d[dye]}/\mathrm{d}t = \frac{2\phi k_1 \mathrm{I}_a[\mathrm{dye}]}{(k_1 - k_2)[\mathrm{dye}] + k_2[\mathrm{dye}]_0} \tag{7}$$

where $[dye]_o$ is the initial dye concentration and $[Int]+[dye]\approx[dye]_o$.

The second order kinetic constant for the hydroxyl radical attack to aromatic compounds is reported to be of the order of 10^9 l mol^{-1} s^{-1} [13,14]. If hydroxyl reactivities towards the different organic compounds present in solution are assumed to be approximately of the same order of magnitude:

$$k_2[\mathrm{dye}]_o >> (k_2 - k_1)[\mathrm{dye}]$$

and Eq. (7) becomes:

$$-\mathrm{d[dye]}/\mathrm{d}t = \frac{2\phi k_1 I_a[\mathrm{dye}]}{k_2[\mathrm{dye}]_0} = \frac{2\phi k_1 I_0[\mathrm{dye}]}{k_2[\mathrm{dye}]_0} F(1-10^{-A}) \tag{8}$$

where F is the fraction of light absorbed by hydrogen peroxide, A is the total absorbance of the solution in the same wavelength range, I_a is the radiation intensity absorbed by the sample and I_o is the intensity of the radiation impinging on the solution.

Under continuous irradiation, due to the high absorbance of the dye, in the initial part of the process, $(1-10^{-A}) \approx 1$ and

$$-\mathrm{d[dye]}/\mathrm{d}t = \frac{2\phi k_1 I_0 F}{k_2[\mathrm{dye}]_0}[\mathrm{dye}] \tag{9}$$

or, more simply,

$$-\mathrm{d[dye]}/\mathrm{d}t = k_{\mathrm{ap}}[\mathrm{dye}] \tag{10}$$

This relationship corresponds to a first order reaction of kinetic constant k_{ap}, which can be obtained by plotting **ln** [dye] as a function of time. The experimental values for the dyes investigated in the present work are reported in Table 1.

Table 1
Kinetic parameters of the degradation process of different dyes

Dye	$k_{ap}(s^{-1})$	k'	t_{max}(min)	$k_{TOC}(s^{-1})$
AR1	8.1×10^{-4}	2.9	40	4.4×10^{-4}
AR40	9.5×10^{-4}	3.2	55	3.3×10^{-4}
MO	10.6×10^{-4}	1.5	60	3.5×10^{-4}
RB19	2.6×10^{-4}	0.8	65	3.6×10^{-4}
AB25	2.8×10^{-4}	1.0	70	5.1×10^{-4}
AB80	5.0×10^{-4}	1.9	120	3.3×10^{-4}
AG27	4.2×10^{-4}	0.7	100	–

Table 2
Kinetic parameters of degradation of AR1 at different pHs

pH	$k_{ap}(s^{-1})$	k'	t_{max} (min)	$k_{TOC}(s^{-1})$
2.8[a]	9.0×10^{-4}	3.3	55	5.6×10^{-4}
6.2[a]	8.1×10^{-4}	2.9	40	4.4×10^{-4}
7.5[b]	10.5×10^{-4}	3.8	40	4.7×10^{-4}
9.2[c]	10.5×10^{-4}	3.8	40	6.1×10^{-4}

[a] Unbuffered solution; pH adjusted by HCl addition; [b] phosphate buffer; [c] borate buffer.

These data are comparable, because the same dye concentration was used for all the experiments; however, different dyes show different UV absorption properties. Thus k_{ap} values can be normalized by taking into account the concentration of the dye and the radiation intensity absorbed by H_2O_2 and by the dye under examination; k' values, obtained as $k' = k_{ap}[\text{dye}]_o/FI_o$, are reported in Table 1. However, it must be noted that F values can be evaluated only approximately and at the beginning of the tests, because the absorption spectra of **Int** and $\mathbf{P_1}$ and the intensity wavelength distribution of lamp emission are unknown. Therefore, k' values should be considered only as a basis for a relative and semiquantitative interpretation of the experimental data.

As stated above, decolorization of test solutions was always accompanied by the formation of fluorescent species. In the case of azo dyes, the emission maxima were at about 450 nm for an excitation wavelength of 366 nm, while in the case of anthraquinone dyes, the corresponding emission and excitation wavelengths were 460 nm and 360 nm, respectively. Table 1 shows the approximate times at which the emission reached a maximum value during the kinetic run (t_{max}).

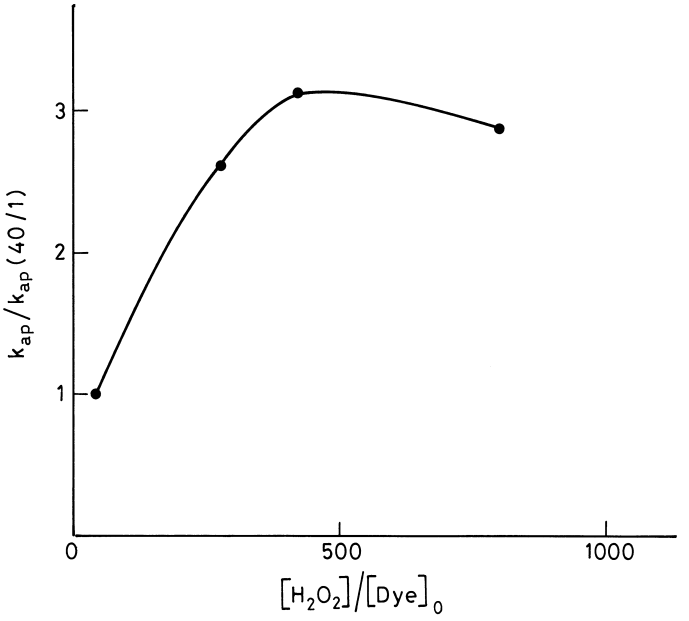

Fig. 8. Effect of hydrogen peroxide concentration on degradation of AR1 by UV/H_2O_2 oxidation.

TOC decay, after the initial slow decrease period, follows, substantially, first order kinetics viz:

$$-\mathrm{d}TOC/dt = k_{\mathrm{TOC}}TOC$$

Experimental k_{TOC} values, determined from the final part of TOC vs time plots, are collected in Table 2. According to the kinetic model of Eqs. (1–6), k_{TOC} is related to k_3.

Thus, as the reported results clearly show, there are no major differences in decolorization and TOC reduction for all the dyes examined. Also, preliminary tests on C.I. Acid Yellow 17 and C.I. Direct Orange 46 have confirmed the general trend.

In order to get a deeper understanding of the process, some further experiments were carried out on AR1. First of all, different $[H_2O_2]$/[dye] ratios were used; the results are reported in Fig. 8. As already observed by other authors [15,16] the decolorization rate increases until it reaches a maximum. Under the adopted conditions, this ratio was around 400/1. The same trend is followed by TOC decay. Secondly, the effect of pH was considered. All the experiments described above were performed in unbuffered solutions; during the process a pH steady decrease , parallel to decolorization, was always observed, as shown in Fig. 9. Some tests were also carried out on AR1 solutions at pH 2.8, 7.5 and 9.2. No pH greater than 9.2 was tested in order to avoid the interference of acid-base equilibria of the dye. The corresponding $k_{\mathrm{ap}}, k', t_{\max}$ and k_{TOC} values, collected in Table 2, show that the general qualitative and kinetic behaviour does not change in the pH range adopted. Finally, sulphate ion concentration was found to increase regularly during the first part of the process (see Fig. 9), while no nitrite or nitrate ions could be found in solution in the same time interval.

These data suggest that the first steps of the oxidative process are represented by the substitution of the sulphonic group, which is present in all the compounds of this present study, and formation of mono- or polyhydroxylated species, some of which are fluorescent. Continuing photooxidation eventually leads to aromatic ring cleavage. As far as the azo group is concerned, it is likely to be transformed in molecular nitrogen at a relatively early reaction stage.

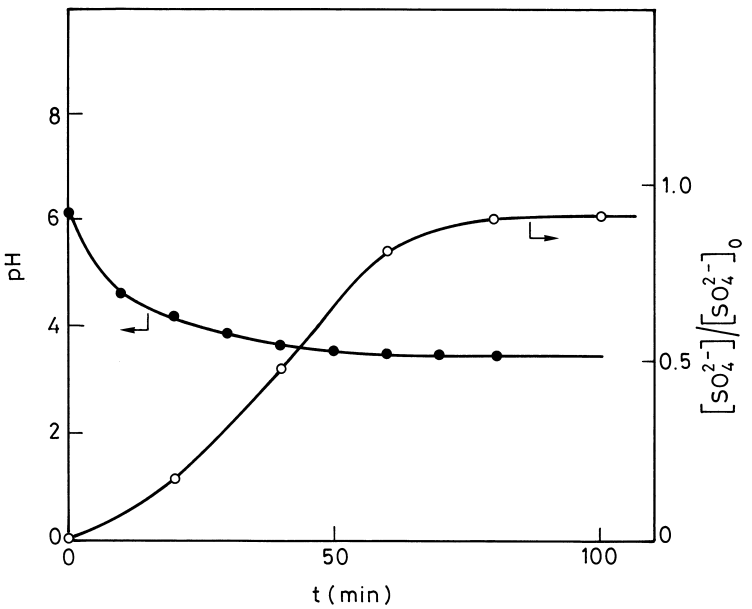

Fig. 9. Changes in pH and sulphate ion concentration as a function of time during degradation of AR1 by UV/H_2O_2 oxidation.

4. Conclusion

The following conclusions can be drawn from the results reported in this work:

1. UV radiation in the presence of hydrogen peroxide leads to complete decolorization and mineralization of sulphonated azo and anthraquinone dyes in a relatively short time. TOC decrease is markedly slower than colour disappearance, but in all cases finally reaches very low values in about 3 h.
2. The process is likely to involve, as a first step, hydroxyl electrophilil addition to the aromatic structure of the dyes, and replacement of the sulphonic acid group. The hydroxylated species so formed show relatively high fluorescence even if the chromogenic structures of the compounds undergo a faster degradation.
3. A simple kinetic model has been proposed which can describe the process in a substantially adequate way. Due to the high reactivity of hydroxyl or other radicals generated during the process, no marked differences can be observed when treating dyes of different chemical structure, at least for the dye classes chosen for this study. Anthraquinone dyes seem to be, in general, a little more resistant to the treatment than azo dyes. An increase in hydrogen peroxide concentration leads to a faster dye degradation until a $[H_2O_2]/[dye]$ ratio of about 400; at higher ratios the degradation process becomes slower.
4. Further research is in progress in order to identify the intermediates, to study possible interferences and/or inhibition by other compounds usually present in dyehouse wastewater, and investigate the effect of radiation intensity and to develop reactors of a more efficient design. In conclusion, UV/H_2O_2 treatment seems a very promising technique for reduction of organic pollutants in industrial wastewaters.

Acknowledgements

This work was in part financially supported by the European Commission (Contract N.BREU.CT. 94.026–ExCOLOUR). We thank L.Bettens (Centexbel) and K.H.Gregor (Solvay S.A.) for helpful discussions.

References

[1] Carey JH. Water Pollution Research Journal, Canada 1992;27:1.
[2] Glaze WH, Beltran F, Tukhanen T, Kang JW. Water Pollution Research Journal, Canada 1992;27:23.
[3] Uygur A. Journal of the Society of Dyers and Colourists 1997;113:211.
[4] Maillard C, Guillard C, Pichet P. Chemosphere 1992; 24:1085.
[5] Nicole I, De Laat J, Doré M, Duguet JP, Bonnel C. Water Research 1990;2:157.
[6] Eisenberg GM. Industrial Engineering Chemistry 1943; 15:327.
[7] Ho PC. Environmental Science and Technology 1986; 20:260.
[8] Guittonneau S, De Laat J, Doré M, Duguet JP, Bonnel C. Environmental Technology Letters 1988;9:1115.
[9] Guittonneau S, De Laat J, Doré M, Duguet JP, Suty H. Environmental Technology 1990;11:57.
[10] Scheck CK, Frimmel FH, Water Research 1995; 29:2346.
[11] Hustert K, Zepp RG. Chemosphere 1992;24:335.
[12] Debellefontaine H, Striolo P, Chakchouk M, Foussard J-N, Besombes-Vailhe J. Revue des Sciences de l'Eau 1992;4:555.
[13] Buxton GV, Greenstock CL, Helman WP, Ross AB. Journal of Physical and Chemical Reference Data 1988;17:513.
[14] Kochany J, Bolton RJ. Environmental Science Technology 1992;26:262.
[15] Shu HY, Huang CR, Chang MC, Chemosphere 1994; 29:2597.
[16] Ince NH, Gönenc DJ, Environmental Technology 1997; 18:179.